



Jacob Friedemann Fast*, Jiazhen He, Michael Jungheim, Tobias Ortmaier, Martin Ptok, and Lüder Alexander Kahrs

An actuated larynx phantom for pre-clinical evaluation of droplet-based reflex-stimulating laryngoscopes

<https://doi.org/10.1515/cdbme-2019-0035>

Abstract: The laryngeal adductor reflex (LAR) is an important protective function of the larynx to prevent aspiration and potentially fatal aspiration pneumonia by rapidly closing the glottis. Recently, a novel method for targeted stimulation and evaluation of the LAR has been proposed to enable non-invasive and reproducible LAR performance grading and to extend the understanding of this reflexive mechanism. The method relies on the laryngoscopically controlled application of accelerated water droplets in association with a high-speed camera system for LAR stimulation site and reflex onset latency identification.

Prototype laryngoscopes destined for this method require validation prior to extensive clinical trials. Furthermore, demonstrations using a realistic phantom could increase patient compliance in future clinical settings. For these purposes, a model of the human larynx including vocal fold actuation for LAR simulation was developed in this work. The combination of image processing based on a custom algorithm and individual motorization of each vocal fold enables spatio-temporal droplet impact detection and controlled vocal fold adduction. To simulate different LAR pathologies, the current implementation allows to individually adjust the reflex onset latency of the ipsi- and contralateral vocal fold with respect to the automatically detected impact location of the droplet as well as the maximum adduction angle of each vocal fold.

An experimental study of the temporal offset between desired and observed LAR onset latency due to image processing was

performed for three average droplet masses based on high-speed recordings of the phantom. Median offsets of 100, 120 and 128 ms were found ($n=16$). This offset most likely has a multifactorial cause (image processing delay, inertia of the mechanical components, droplet motion). The observed offset increased with increasing droplet mass, as fluid oscillations after impact may have been detected as motion. In future work, alternative methods for droplet impact detection could be explored and the observed offset could be used for compensation of this undesirable delay.

Keywords: Laryngeal adductor reflex, laryngoscope development, anatomical model, MIT-LAR.

1 Introduction

Besides its function in voice production, the larynx plays a vital role in airway protection. The laryngeal adductor reflex (LAR) prevents the intrusion of matter into the trachea by a quick adduction of the vocal folds [11]. A pathological LAR is thought to increase the risk of aspiration pneumonia [10]. Thus, a non-invasive and objective method for routine LAR performance screening should be established. The LAR onset latency Δt_{LAR} , defined with the stimulation instant t_1 and the adduction onset instant t_2 as $\Delta t_{\text{LAR}} = t_2 - t_1$, is thought to be a good indicator of LAR performance [9]. It has been shown previously that accelerated droplets are suitable for noninvasive LAR triggering [9]. A commercially available high-speed laryngoscope was combined with a droplet applicator module to perform Microdroplet Impulse Testing of the LAR (MIT-LAR) [9]. In previous work, a mechatronic system was designed to control droplet formation [5]. An enhanced MIT-LAR laryngoscope with stereoscopic droplet impact site prediction was developed [4].

To assess the performance of such novel MIT-LAR devices prior to extensive clinical trials, a test setup showing a LAR response comparable to human behavior is highly desirable. Therefore, an actuated phantom of the human larynx including a function for droplet impact detection and simulation of the LAR response is presented in this contribution. The

*Corresponding author: **Jacob Friedemann Fast**, Leibniz Universität Hannover, Institute of Mechatronic Systems, Appelstr. 11a, 30167 Hannover, Germany, e-mail: jacob.fast@imes.uni-hannover.de

Jiazhen He, Tobias Ortmaier, Leibniz Universität Hannover, Institute of Mechatronic Systems, Hannover, Germany

Michael Jungheim, Martin Ptok, Hannover Medical School, Department of Phoniatrics and Pediatric Audiology, Carl-Neuberg-Str. 1, 30625 Hannover, Germany

Lüder Alexander Kahrs, Center for Image Guided Innovation and Therapeutic Intervention (CIGITI), The Hospital for Sick Children, 555 University Ave, Toronto, ON M5G 1X8, Canada

Lüder Alexander Kahrs, Department of Mathematical and Computational Sciences, University of Toronto Mississauga, 3359 Mississauga Rd, Mississauga, ON L5L 1C6, Canada

assembly could also be used for demonstration purposes in a clinical setting to enhance patient compliance.

2 Materials and methods

The following anatomical and physiological aspects are required to obtain a device that is considered helpful for the assessment of prototypical MIT-LAR laryngoscopes in a lab setting:

- anatomical reproduction of laryngeal structures,
- imitation of physiological and pathological LAR response patterns
- variation of response latencies for the ipsi- and contralateral vocal fold with respect to the stimulus.

This section summarizes the methods to achieve an anatomically correct shape of the LAR phantom, the concept and realization of a physiological actuation of the phantom and the experimental procedure for a first system performance evaluation.

2.1 Anatomical reproduction of laryngeal structures

The thyroid cartilage is the largest cartilage of the larynx and anteriorly encloses the vocal folds. To obtain an anatomically correct shape of the thyroid cartilage, a volumetric model derived from magnetic resonance imaging scans was used [12]. It was manufactured by 3D printing (Objet 350 Connex 3, Stratasys, Ltd., Eden Prairie, USA) at a scale factor of 200 % to facilitate component integration. A coating of colored silicone (Ecoflex™ 00-30 silicone with Silc Pig® coloring agent, Smooth-On, Inc., Macungie, USA) was applied to the replicated cartilage in order to obtain a more realistic surface texture. The vocal folds were modeled by curved plates and 3D printed. The length and width of these plates were set approximately to the average literature values for men (scale factor: 200 %) found in [3]. The artificial vocal folds were coated in colored silicone and a slight vascular pattern was added manually.

2.2 Imitation of LAR response patterns

In order to enable a realistic simulation of the LAR in response to a droplet impact as during MIT-LAR, a sensor concept for droplet impact detection was developed and integrated into the phantom.

A single-board computer (Raspberry Pi 3 B+, Raspberry Pi Trading Ltd., Cambridge, UK) running the open-source operating system Raspbian Stretch was used to execute the algorithm shown in Fig. 1, implemented in C++ using the open-source image processing library OpenCV 3 [2]. A camera module (OV 5647, OmniVision Technologies, Inc., Santa Clara, USA), mounted above the LAR phantom, was used as optical sensor. The algorithm for droplet impact detection is shown as a simplified flow diagram in Fig. 1.

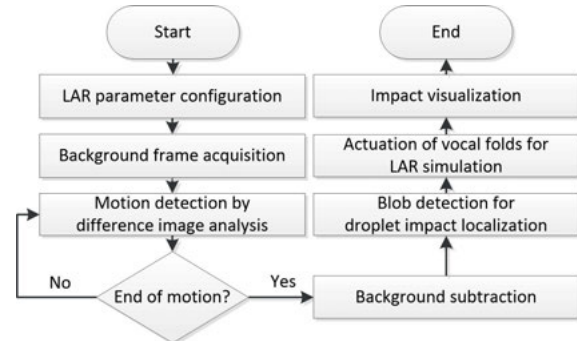


Fig. 1: Flow diagram for droplet impact detection and phantom actuation.

Various concepts for larynx phantom actuation can be found in literature. *Ex vivo* assemblies based on the integration of animal larynges were proposed [1]. However, this approach was deemed unsuitable for the purpose of the present work due to the limited durability and availability of animal larynges. Assemblies relying on synthetic models are destined for oscillation studies and do not provide LAR simulation capabilities [6, 7, 13].

Manti et al. proposed a biorobotic assembly featuring a spring and actuation cables to control the degree of adduction [8]. Although the proposed setup was intended for phonation experiments, a similar principle was applied in this work to achieve LAR-like motion. Each vocal fold was anteriorly mounted to a pivotal rod and actuated by a lever connected to a servomotor positioned laterally to the thyroid cartilage. The overall setup developed in this work is shown in Fig. 2. To enable simulation of pathological LAR phenotypes, a graphical user interface was implemented to independently configure the rotation onset latency as well as the angle of rotation for each vocal fold. The impacted side of the phantom was automatically identified by blob detection (cf. Fig. 1). The source code of the proposed algorithm can be found here: https://github.com/JFast/LAR_phantom.

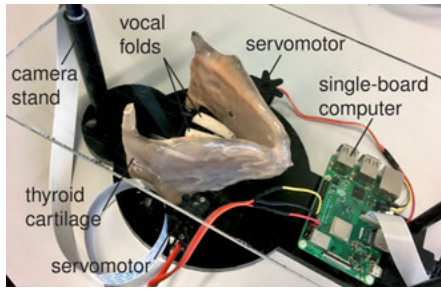


Fig. 2: Components of LAR phantom developed in this work.

2.3 Experimental study of system performance

A mixture of distilled water, sodium chloride (Südwestdeutsche Salzwerke AG, Heilbronn, Germany) at a concentration of 5 mol per liter of water and food colorant E 150c (Appel Feinkost GmbH & Co. KG, Cuxhaven, Germany) at a concentration of 5% (V/V) with respect to the volume of water before salt addition was used as working fluid. This mixture contains only nontoxic additives and has been shown to enable stable droplet formation.

The desired reflex onset latency was set to a constant value of 100 ms for all experiments, a value that is in good accordance with the average value of 106 ms reported for the optically determined LAR onset latency in a first MIT-LAR pilot study [9]. Droplets were shot on the larynx phantom using the droplet applicator module from the MIT-LAR stereolaryngoscope presented previously [4]. A high-speed camera (Os^v37-S1, IDT Inc., Pasadena, USA) was used at a frame rate of 1000 fps to record the phantom's motion in response to droplet impact events. The experimental setup is shown in Fig. 3. The rate of non-identified droplet impacts was determined for each average droplet mass (low, medium and high) with a sample size of $n = 20$.

Additional sequences were recorded to obtain a minimum sample size of $n = 16$ for manual quantification of the temporal offset between droplet impact and start of vocal fold rotation. The open-source video processing application Avidemux 2.7.0 was employed for this analysis.

3 Results

The temporal offset between the set and observed LAR onset latency is given in Fig. 4 for three average droplet masses. For the intermediate droplet mass, two extreme outliers (344 ms and 513 ms) are not shown in the plot due to axis scaling. The percentage of non-identified impacts in percent as well as the



Fig. 3: Setup for system performance evaluation.

median offset between set and experimentally found LAR onset latency in milliseconds are shown in Tab. 1. The maximum percentage of silent impacts found in a MIT-LAR pilot study with 10 subjects is included for comparison [9].

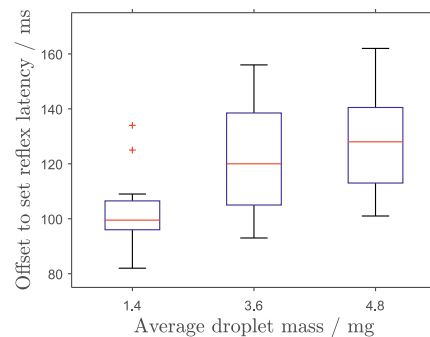


Fig. 4: Offset between set and observed LAR onset latency for different average droplet masses ($n=16$). Two outliers not shown due to axis scaling (see text).

4 Discussion

Using an optical droplet impact detection method, a versatile and customizable setup for pre-clinical evaluation of prototypes of MIT-LAR laryngoscopes was achieved. The experimental study indicates an offset between set and observed Δt_{LAR} as droplet impact detection and servomotor actuation have to be processed by the single-board computer. The

Tab. 1: Summary of LAR phantom performance assessment results and comparison with MIT-LAR pilot study results [9].

Droplet mass	Silent impacts in % (n=20)	Median offset in ms (n=16)
Low	30	100
Medium	5	120
High	10	128
MIT-LAR pilot study [9]	up to 83.4 (n differing)	not applicable

offset tends to increase with increasing droplet mass. This can be explained by the difference image analysis method used for droplet impact detection, as bigger drops oscillate longer after impact. On the other hand, bigger drops yield higher detection rates as they are more reliably detected by difference image analysis.

A response rate below 100 % is in good accordance with the results of a MIT-LAR pilot study, where LAR response rates as low as 16.6 % were found optically when stimulating the right side of the piriform recess [9].

5 Outlook

The setup presented in this work shows a relatively high rate of non-detected droplet impacts. This behavior was also found in a pilot study with 10 test persons [9]. To enable an even more realistic LAR behavior, a sensor for impact intensity measurement could be added. The proposed setup will be revised to offer a more and more precise droplet impact detection to keep up with future MIT-LAR laryngoscopes. The results of this work will be helpful to achieve a more accurate LAR onset latency by compensating the observed delay introduced by image processing.

Acknowledgment: J. F. F. acknowledges Caroline Bärhold for providing an extensive overview of recent research in the field of larynx models and Adrian Karl Ruppel for his contributions to the motion detection method used in this work.

Author Statement

Research funding: This work has been funded by Deutsche Forschungsgemeinschaft (DFG) grants KA 2975/6-1 and PT 2/5-1. Conflict of interest: Authors state no conflict of interest. Ethical approval: The conducted research is not related to either human or animals use.

References

- [1] V. Birk, M. Döllinger, A. Sutor, D. A. Berry, D. Gedeon, M. Traxdorf, O. Wendler, C. Bohr, and S. Kniesburges. Automated setup for ex vivo larynx experiments. *J Acoust Soc Am*, 141(3):1349, 2017. ISSN 0001-4966. 10.1121/1.4976085.
- [2] G. Bradski. The OpenCV Library. *Dr. Dobb's Journal of Software Tools*, 2000.
- [3] H. E. Eckel, C. Sittel, P. Zorowka, and A. Jerke. Dimensions of the laryngeal framework in adults. *Surg Radiol Anat*, 16 (1994):31–36, 1994.
- [4] J. F. Fast, A. K. Ruppel, C. Bärhold, M. Jungheim, T. Ortmaier, M. Ptok, and L. A. Kahrs. Endoscopic guidance system for stimulation of the laryngeal adductor reflex by droplet impact. In B. Fei and C. A. Linte, editors, *Medical Imaging 2019: Image-Guided Procedures, Robotic Interventions, and Modeling*, page 21. SPIE, 2/16/2019 - 2/21/2019. ISBN 9781510625495. 10.1117/12.2512852.
- [5] J. F. Fast, A. Muley, D. Kühn, F. Meisoll, T. Ortmaier, M. Jungheim, M. Ptok, and L. A. Kahrs. Towards microprocessor-based control of droplet parameters for endoscopic laryngeal adductor reflex triggering. *Current Directions in Biomedical Engineering*, 3(2):239–243, 2017. 10.1515/cdbme-2017-0050.
- [6] M. Krane, M. Barry, and T. Wei. Unsteady behavior of flow in a scaled-up vocal folds model. *J Acoust Soc Am*, 122(6): 3659–3670, 2007. ISSN 0001-4966. 10.1121/1.2409485.
- [7] B. R. Kucinschi, R. C. Scherer, K. J. Dewitt, and T. T. M. Ng. An experimental analysis of the pressures and flows within a driven mechanical model of phonation. *J Acoust Soc Am*, 119(5 Pt 1):3011–3021, 2006. ISSN 0001-4966. 10.1121/1.2186429.
- [8] M. Manti, M. Cianchetti, A. Nacci, F. Ursino, and C. Laschi. A biorobotic model of the human larynx. In *Proceedings of the Annual International Conference of the IEEE Engineering in Medicine and Biology Society, EMBS*, volume 2015-November, pages 3623–3626. 2015. ISBN 9781424492718. 10.1109/EMBC.2015.7319177.
- [9] M. Ptok and S. Schroeter. Charakterisierung des laryngealen Adduktionsreflexes durch Stimulation mit Mikrotröpfchen-Impulsen (microdroplet impulse testing). *Laryngol Rhinol Otol*, 95(7):482–489, 2016. 10.1055/s-0041-111516.
- [10] M. Ptok, S. Bonenberger, S. Miller, D. Kühn, and M. Jungheim. Der laryngeale Adduktionsreflex. *Laryngol Rhinol Otol*, 93(7):446–449, 2014. 10.1055/s-0034-1370928.
- [11] C. T. Sasaki and M. Suzuki. Laryngeal reflexes in cat, dog, and man. *Arch Otolaryngol*, 102(7):400–402, 1976. ISSN 00039977. 10.1001/archotol.1976.00780120048004.
- [12] W. S. Selbie, S. L. Gewalt, and C. L. Ludlow. Developing an anatomical model of the human laryngeal cartilages from magnetic resonance imaging. *J Acoust Soc Am*, 112(3 Pt 1): 1077–1090, 2002. ISSN 00014966.
- [13] M. Triep, C. Brücker, and W. Schröder. High-speed PIV measurements of the flow downstream of a dynamic mechanical model of the human vocal folds. *Exp Fluids*, 39(2):232–245, 2005. ISSN 0723-4864. 10.1007/s00348-005-1015-3.